Biochimica et Biophysica Acta 1807 (2011) 1075–1082

Contents lists available at ScienceDirect

Biochimica et Biophysica Acta

journal homepage: www.elsevier.com/locate/bbabio

Inhibition of proton pumping in membrane reconstituted bovine heart cytochrome *c* oxidase by zinc binding at the inner matrix side

Pietro Luca Martino [a], Giuseppe Capitanio [a], Nazzareno Capitanio [b], Sergio Papa [a,c,*]

[a] Department of Medical Biochemistry, Biology and Physics, University of Bari, Bari, Italy
[b] Department of Biomedical Sciences, University of Foggia, Foggia, Italy
[c] Institute of Bioenergetics and Biomembranes, CNR, Bari, Italy

ARTICLE INFO

Article history:
Received 18 March 2011
Received in revised form 13 May 2011
Accepted 16 May 2011
Available online 26 May 2011

Keywords:
Cytochrome *c* oxidase
Proton pumping
Redox Bohr effect
Allosteric cooperativity
Zinc inhibition

ABSTRACT

A study is presented on the effect of zinc binding at the matrix side, on the proton pump of purified liposome reconstituted bovine heart cytochrome *c* oxidase (COV). Internally trapped Zn^{2+} resulted in 50% decoupling of the proton pump at level flow. Analysis of the pH dependence of inhibition by internal Zn^{2+} of proton release in the oxidative and reductive phases of the catalytic cycle of cytochrome *c* oxidase indicates that Zn^{2+} suppresses two of the four proton pumping steps in the cycle, those taking place when the 2 OH^- produced in the reduction of O_2 at the binuclear center are protonated to 2 H_2O. This decoupling effect could be associated with Zn^{2+} induced conformational alteration of an acid/base cluster linked to heme a_3.

1. Introduction

Cytochrome *c* oxidase, the terminal aa_3–copper oxygen reductase of eukaryotic and prokaryotic respiratory chain has four redox centers: a binuclear Cu_A, titrating as one electron transfer center, bound to subunit II at the outer (P) surface of the membrane embedded oxidase, heme *a*, heme a_3 and Cu_B all these bound to subunit I in a location close to the outer surface [1,2]. Cytochrome *c*, at the outer (P) side of the membrane, shuttling between the bc_1 cytochrome *c* reductase and cytochrome *c* oxidase, delivers electron to Cu_A, heme *a* transfers electrons from Cu_A to the heme a_3–Cu_B binuclear center, where O_2 is reduced to 2 H_2O with consumption of 4 H^+ from the inner (N) space [3,4] with direct generation of transmembrane $\Delta\mu H^+$ (Reaction 1).

$$4\ \text{cyt}\ c^{2+} + 8\ H^+_N + O_2 \rightarrow 4\ \text{cyt}\ c^{3+} + 2\ H_2O + 4\ H^+_P \qquad (1)$$

In addition, up to four protons are pumped from the N to the outer P space in the reduction of O_2 to 2 H_2O by cytochrome *c* (Reaction 1) [5,6]. Since there are no hydrogen carriers in the oxidase, proton pumping has to involve thermodynamic cooperative linkage between electron transfer at the metal centers and proton translocation at acid/base groups in the enzyme (Redox Bohr protons) [4,7].

The bovine heart enzyme has, in addition to the conserved subunits I, II and III, 10 supernumerary subunits. Mutational analysis (see ref. [8] for review) and X-ray crystallographic structures [1,2] have identified two conserved proton translocation pathways in subunit I of cytochrome *c* oxidase, K and D pathways. The K pathway mediates the conduction from the N space to the a_3–Cu_B binuclear center of two of the four scalar protons consumed in the reduction of O_2 to 2 H_2O [1,2,9–11]. The other two scalar protons consumed in H_2O formation are conducted from the N space to the binuclear center by the D pathway [1,2,9–11]. This appears to be involved, at least in the prokaryotic oxidases, also in the translocation of the four pumped protons from the N space to the coupling site of the proton pump [9–13]. X-ray crystallographic structure of the bovine oxidase shows also an additional H proton conducting pathway, with a water channel conducting protons from the N space to the environment of heme *a* and a hydrogen bond pathway conducting protons from this to the P space [2,14].

The current models of proton pumping in the oxidase can be grouped in two types: (i) those in which the cooperative coupling is conceived to be directly associated with the heme a_3–Cu_B binuclear site where O_2 is reduced to H_2O [11,13] and (ii) those in which cooperative proton transfer linked to electron transfer at heme *a* plays a key role in the pump [5,14–25].

Abbreviations: COX, purified cytochrome *c* oxidase; COV, cytochrome *c* oxidase reconstituted in phospholipid vesicles; Hepes, 4-(2-hydroxyethyl)-1-piperazineethanesulfonic acid; Tris, tris(hydroxymethyl)-aminometane; Mes, 2-morpholinoethanesulfonic acid; EDTA, ethylendiaminetetracetic acid; FIC, potassium ferricyanide; CCCP, carbonyl cyanide 3-chloro-phenylhydrazone; BHM, frozen–thawed beef heart mitochondria; R, fully reduced cytochrome *c* oxidase; O, fully oxidized cytochrome *c* oxidase; MV, mixed valence state; P_M, peroxy state; F, ferryl state

* Corresponding author at: Department of Medical Biochemistry, Biology and Physics, University of Bari, Policlinico, P.zza G. Cesare, 70124 Bari, Italy. Tel.: + 39 080 5448541; fax + 39 080 5448538.
E-mail address: s.papa@biochem.uniba.it (S. Papa).

0005-2728/$ – see front matter © 2011 Elsevier B.V. All rights reserved.
doi:10.1016/j.bbabio.2011.05.015

Redox Bohr protons linked to heme a (Cu_A) and Cu_B have been found to display vectorial nature, i.e., they are taken up from the inner (N) space upon reduction of the metals and released in the outer (P) space upon their oxidation. Redox Bohr protons linked to oxido-reduction of heme a_3 have been found, instead, to be scalar, i.e., exchanged only at the outer (P) space [17,18].

Work from various laboratories has shown that exogenous zinc inhibits the respiratory activity of cytochrome *c* oxidase [26,27] and impairs proton pumping [27–33]. These inhibitory effects appear to be associated with exogenous zinc binding at the inner N-side and the outer P-side [30,31], respectively. EXAFS [33] and X-ray crystallographic analysis [34] have identified residues in subunits I, III and VII_c of bovine cytochrome *c* oxidase involved in the binding of zinc at the inner entry mouth of the D pathway. The zinc binding at the N-side appears to be responsible for uncoupling of proton pumping under conditions in which there is small inhibition of electron transfer [28,33].

In this paper a study is presented on the effect of internally trapped zinc on the proton pump of purified liposome reconstituted bovine heart cytochrome *c* oxidase (COV). This Zn^{2+} binding at the N-side of the oxidase results in 50% decoupling of the proton pump at level flow. The pH dependence of the inhibition by internal Zn^{2+} of proton release in the oxidative and reductive phases of cytochrome *c* oxidase cycle [9,24,35] indicates that Zn^{2+} suppresses two of the four proton pumping steps in the catalytic cycle of O_2 reduction to 2 H_2O [24]. Zn^{2+} causes also depression of Bohr protons linked to heme a_3.

2. Materials and methods

2.1. Materials

Horse heart cytochrome *c* (type VI), valinomycin, rotenone, riboflavin, EDTA, phospholipid (L-α-Lecithin, L-α-Phosphatidylcholine, type II-S: from soybean), catalase, superoxide dismutase, antimycin A, myxothiazol and CCCP were from Sigma Chemical Co., potassium ferricyanide from BDH Chemicals Ltd. All other reagents were of the highest purity grade commercially available.

2.2. Enzyme preparation and reconstitution in liposomes

Cytochrome *c* oxidase was purified from beef heart mitochondria as described in [36]. The nmoles of heme $a + a_3$/mg protein were about 10 and SDS-PAGE analysis revealed the complete set of 13 subunits [37]. The activity of the enzyme preparation measured polarographically in 40 mM KCl, 3.4 mM Hepes, 3.1 mM Tris, 3.5 mM MES, 0.1 mM EDTA, 50 μM cytochrome *c*, and 40 nM aa_3, supplemented with 25 mM ascorbate was, at room temperature, never below 70 O_2 molecules $s^{-1} aa_3^{-1}$. The oxidase vesicles, 1 mg prot. COX and 40 mg of sonicated phospholipids, were sealed by cholate dialysis [6] in a mixture of 34 mM Hepes, 31 mM Tris, 35 mM MES at the pHs specified in the figures. The buffer capacity of this mixture (β) was 25 mM H^+/ΔpH unit in the pH range from 6.5 to 8.5. The percentage of total cytochrome *c* oxidase incorporated "right-side out" calculated after reduction by impermeant and permeant reducing agents in presence of cyanide was never below 85%. The respiratory control ratio (rate of electron flow in the presence of valinomycin plus CCCP/rate of electron in their absence), measured polarographically [6] at each pH, was never lower than 12. Where indicated, $ZnCl_2$ (200 μM) was added to the sonication medium and to the first two dialysis solutions but omitted from the third in which EDTA was added to chelate external Zn^{2+}. The membrane orientation of the oxidase was not affected when the enzyme was incorporated in liposomes in the presence of $ZnCl_2$[33]. The presence of $ZnCl_2$ during liposome reconstitution of cytochrome *c* oxidase had no effect on the respiratory control ratio nor increased the residual amount of soluble COX [33]. To prepare CO-ligated cytochrome *c* oxidase, the suspension placed in the cuvette was gently bubbled with CO for 2–3 min and then the cuvette connected to the oxygen-trapping device. Addition of 2 mM succinate in the presence of a trace of disrupted (BHM) and cytochrome *c* produced anaerobiosis and full reduction of cytochrome *c* oxidase in 10–15 min with its characteristic spectrum generated by CO binding to the reduced enzyme [17]; in this condition heme a_3 and Cu_B are blocked in the reduced state [38]. In order to obtain the CN-ligated oxidase, the enzyme reconstituted in liposomes was incubated overnight in 6–15 mM KCN, depending on pH, at 4 °C and the typical Soret shift from 420–422 nm to 428 nm in the treated oxidized enzyme was obtained [39]; in this condition, heme a_3 is blocked in the oxidized state [40].

2.3. Measurement of redox-linked proton translocation in COV under level flow conditions

Redox-linked translocation under "level flow" conditions was measured according to the method described in refs. [41,42]. The initial rates of pH changes and O_2 consumption, elicited upon activation of electron flow in COV suspension, was estimated spectrophotometrically from the absorbance changes of the phenol red indicator (558–593 nm) and deoxygenation of added oxyhemoglobin (577–568 nm, $\Delta\varepsilon = 6.3\ mM^{-1}\ cm^{-1}$), respectively.

2.4. Measurement of pH and redox changes in aerobic oxidation and reduction phases of COV and in anaerobic oxidation and oxido-reduction of unligated, CN-ligated and CO-ligated COV

Liposome-reconstituted oxidase (COV) was suspended at a final concentration of 1–1.5 μM aa_3 in 150 mM KCl. The reaction medium was made almost completely anaerobic in the cell of an oxygraph, where the oxygen concentration was checked potentiometrically (Clark-type electrode), before being introduced in the measuring cuvette under argon flux. The COV suspension filled in a spectrophotometric thermostated quartz cuvette, with a square cross section of 1 cm^2, was vigorously stirred using a glass-covered magnetic bar. The top of the cuvette was sealed with a stainless steel stopper having a port for the pH electrode, two small holes for injection needles and a port for the entry of argon. Residual oxygen was removed from the argon by passing the gas through oxygen-trapping columns (R&D Separation, OT 3–4 and LIOT 4). The gas path was made of glass or stainless steel narrow tubings connected by teflon Swagelok ferrules. In order to minimize evaporation of the sample, argon was passed through two successive water-filled bubblers. Injections of air saturated H_2O and chemicals were made using gas-tight syringes (Hamilton) driven by a computer-controlled titration–injection pump (Oroboros Instruments). Simultaneous recording of absorbance and pH changes were carried out with a diode-array spectrophotometer (settled in the multiwavelength mode) and a combined pH electrode with accuracy of 5×10^{-4} absorbance and 10^{-3} pH unit respectively (overall response time < 1 s) [43]. The wavelengths selected were 550–540 nm for cytochrome *c*, 445–470 nm and 605–630 nm for heme a_3 and heme *a* in the unligated enzyme. The concentration of aa_3 was determined using a μM extinction coefficient at 445–470 nm of 0.188 cm^{-1} for heme aa_3[44,45]. In the CN-inhibited cytochrome *c* oxidase, redox changes of heme *a* were monitored using a $\Delta\varepsilon$ at 605–630 of 21.6 mM^{-1} assuming 80% contribution of heme *a* to the overall absorbance, at the indicated wavelength couple, in the unligated state [46]. In the CO-ligated state heme *a* oxidation was followed at 604–630 nm ($\Delta\varepsilon = 21.9\ mM^{-1}$), and the generation of the mixed valence state at 590–630 nm ($\Delta\varepsilon = 10.0\ mM^{-1}$) [38]. Ferricyanide concentration was determined at 420–500 nm using a $\Delta\varepsilon$ of 1.0 mM^{-1}. All the measurements were carried out at 25 °C.

2.5. Metal analysis and determination of trapped volume

The inner concentration of $ZnCl_2$ in the liposomes was determined by inductively coupled plasma optical emission spectroscopy (ICP-OES, JOBIN YVON JY 24R). The internal volume of the vesicles was calculated by entrapping phenol red within the liposomes. The dye was added at a

concentration of 100 μM prior to sonication and into the first two dialysis steps and was absent into the last two dialysis steps. Relative phenol red concentrations were determined by measuring the absorbance at 558–593 nm. Measurement of [Zn^{2+}_i] by ICP-OES showed that the absolute amount of zinc present after dialysis was about 12 times lower than that added initially. This was in good agreement with the result of the calculation of the average internal volume of the vesicles that was estimated to be about 7.5% of the total volume.

3. Results

3.1. Effect of internal Zn^{2+} on proton pumping and respiratory activity in liposome reconstituted cytochrome c oxidase (COV) under level flow conditions

The effect of Zn^{2+}, entrapped inside the cytochrome *c* oxidase liposomes (COV), on respiratory rate and H^+ release under level flow conditions is presented in Table 1. The H^+/e^- ratio for proton pumping at level flow, in the presence of valinomycin plus K^+[6], to abolish back-pressure by the ensuing membrane potential generated by proton pumping, was obtained from the initial rates of H^+ release and O_2 consumption initiated by ferricytochrome *c* addition to COV supplemented with Ascorbate plus TMPD. 200 μM Zn^{2+} caused 50% decrease of the rate of H^+ release with no inhibitory effect, under these conditions, on the respiratory rate and the respiratory control ratio (see however [27,28]).

3.2. The effect of Zn^{2+} on proton translocation in the oxidative and reductive phases of the oxidase

The effect of internally trapped Zn^{2+} on proton release from COV in the oxidation and reduction of the oxidase was directly analyzed (Fig. 1). Oxidation of the fully pre-reduced oxidase was produced by the addition of a slightly substoichiometric amount of O_2. The H^+/COX ratio for proton release from COV, in the oxidative phase, pointing to ≈3 at acidic pH decreased to around 2, at alkaline pHs (Fig. 1, filled squares) [24]. Zn^{2+} inhibited H^+ release, which now resulted in an H^+/COX ratio of 1.2–1.3 in the pH range examined (Fig. 1, empty squares). The reductive phase of COV, obtained by ascorbate reduction of the fully oxidized enzyme, resulted in proton release

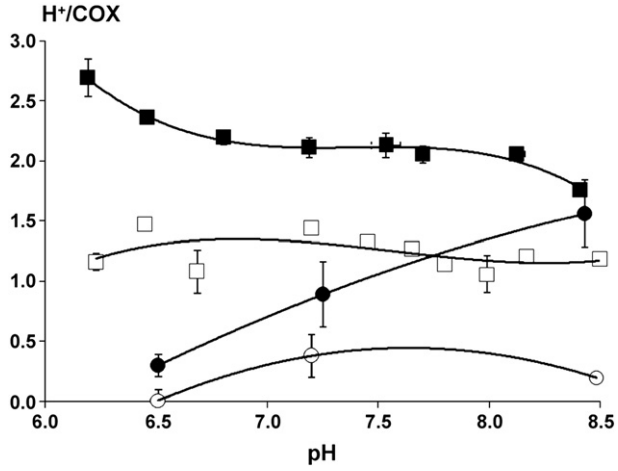

Fig. 1. pH dependence of proton release in the oxidation of fully reduced oxidase and its reduction in COV. COV (1–1.5 μM) were suspended in 150 mM KCl at various pHs, supplemented with 4 μM valinomycin. The pH changes associated with redox transitions of the metal centers in COX were measured potentiometrically and calibrated with anaerobic titrated HCl and KOH solutions. In the oxidation transition (squares), anaerobic full reduction of cytochrome *c* oxidase was attained by the photo-activated EDTA/riboflavin system, in the presence of 1 mM EDTA, 0.1 μM riboflavin [47], 0.05 μM cytochrome *c*, with repetitive flashes of actinic light (100 ms, 3000 lm). 30 μg SOD and 3000 U catalase were also added to 1 ml of the suspending medium in order to remove oxygen free radicals eventually produced by direct reduction of oxygen by riboflavin during flashes. No further electron delivery to the oxidase takes place in the absence of flashes [47]. The fully reduced oxidase was oxidized by the addition of few microliters of air-equilibrated water containing a number of O_2 electron equivalents slightly substoicheiometric with those of the four redox centers of the oxidase [44]. The H^+/COX ratios were obtained by dividing the amount of proton release by that of the COX oxidized. Filled squares: H^+/COX ratios (n = 1–5 ± S.E.M.) from control COVs; empty squares: H^+/COX ratios (n = 1–3 ± S.E.M.) from COV with 200 μM of internally trapped Zn^{2+}. In the reduction transition (circles), after photoreduction in anaerobiosis of a small amount of the oxidase with the EDTA/riboflavin system (the absence of O_2 in the sample was verified by the absence of COX reoxidation), complete reduction of cytochrome *c* oxidase, supplemented with 1.5 μM cytochrome *c*, was produced by the addition of 2 mM anaerobic ascorbate. Upon achievement of full reduction of COX a second pulse of ascorbate was made. The H^+/COX ratio was obtained by subtracting from the pH change caused by the first ascorbate pulse, the artifactual pH change observed upon the second ascorbate pulse. The H^+ release thus calculated was corrected for the scalar H^+ release directly arising from the oxidation of ascorbate to dehydroascorbate equal to 0.5 × (Σ COX metal centers plus cytochrome *c* reduced) [44]. Filled circles: H^+/COX ratios (n = 3–4 ± S.E.M.) from control COV; empty circles: H^+/COX ratios (n = 3–5 ± S.E.M.) from COV with 200 μM internally trapped Zn^{2+}. For other details, see Section 2.

Table 1
Effect of internal Zn^{2+} on proton pumping and respiratory activity in liposome reconstituted cytochrome c oxidase (COV) under level flow condition.

	μM e^-/min	RCR	H^+/e^-
Control	118.35 ± 2.4	25.15 ± 1.4	0.76 ± 0.06
+ $ZnCl_2$ 200 μM	126.85 ± 2.4	23.27 ± 1.1	0.41 ± 0.05*
+ $ZnCl_2$ 500 μM	119.73 ± 2.5	19.71 ± 1.6	0.39 ± 0.02*

Cytochrome c oxidase vesicles (0.35 μM aa_3 final concentration) were suspended in a buffer containing 100 mM Choline–Cl, 5 mM KCl, 1 mM EDTA, 2 μg valinomycin/mL, pH 7.2. For pH measurements the medium was supplemented with 50 μM phenol red and the absorbance changes (at 558–593 nm) were calibrated with standard solutions of 10 mM HCl and KOH; for O_2 consumption measurements the medium was supplemented with 30 μM purified human hemoglobin (factor *f* for the preparation used was 1.6 at pH 7.2; see ref.[41]). The oxygen concentration was lowered by a stream of argon until absorbance changes at 577–568 nm showed that hemoglobin was 50% deoxygenated (for details of the procedure see ref. [41]). The reaction was started by pulsing 0.4 μM ferricytochrome *c* in the presence of 7 mM of Ascorbate plus 35 μM TMPD. The H^+/e^- ratio was measured from the initial rates of proton release and O_2 uptake; H^+ release was corrected for the scalar proton release associated with the oxidation of ascorbate to dehydroascorbate (i.e., 0.5 H^+/e^-). The initial rates of e^- transfer to O_2 (μM e^-/min) and the resulting $H^+/e^-$are presented in the Table. RCR: respiratory control ratio (rate of electron flow in the presence of valinomycin plus CCCP/rate of electron in their absence). The table summarizes the statistical analysis of 4–5 measurements ± S.E.M. under each condition from different proteoliposome preparations. *P<0.01 with respect to control. For other details, see Section 2.

with an H^+/COX ratio which increased progressively with the pH from around 0.3 at pH 6.5 to 1.6 at pH 8.5 (Fig. 1, filled circles). Zn^{2+} caused practically complete suppression of the H^+ release associated with the reductive phase (Fig. 1, empty circles).

3.3. The effect of Zn^{2+} on redox Bohr protons coupled to anaerobic oxido-reduction of metal centers of the oxidase

Bohr protons associated with oxido-reduction of the metal centers of the oxidase, in the absence of additional contributions by intermediates of the oxygen reduction cycle, were analyzed by measuring the H^+ release from COV induced by anaerobic ferricyanide oxidation of the fully reduced oxidase. Fig. 2 shows the actual measurements of cytochrome *c* oxidase (and added cytochrome *c*) reduction/oxidation and the oxidation-linked H^+ release from COV at pH 7.2. Full reduction of 1 μM aa_3 and 1.5 μM cytochrome *c* corresponded to the reduction of 5.5 μequivalents (four metal centers in the oxidase plus 1.5 cytochrome *c*). Anaerobic oxidation of the metal centers was produced by the addition of 5.2 μM ferricyanide (slightly substoicheiometric to avoid undesidered eventual oxidation of unknown components). 1.63 H^+/COX were released in the external medium. In the presence of internally trapped Zn^{2+} and under the same experimental conditions of

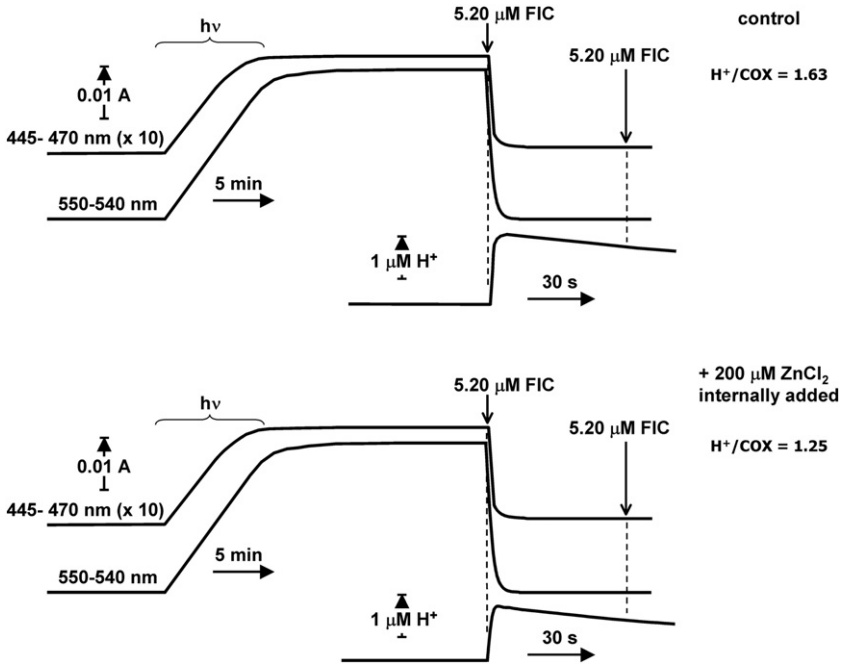

Fig. 2. Proton release and redox changes of aa_3 in anaerobic oxidation by ferricyanide of unligated COV. 1 μM aa_3 plus 1.5 μM cytohcrome *c* were suspended in 150 mM KCl, 1 mM EDTA supplemented with 4 μM valinomycin, pH 7.2, 25 °C. Where indicated, COV were prepared in the presence of $ZnCl_2$. The reduction and subsequence oxidation of the oxidase and cytochrome *c* were directly measured spectrophotometrically as described in Section 2. Anaerobic reduction of cytochrome *c* oxidase and cytochrome *c* was produced by riboflavin/EDTA-mediated photoreduction as described in legend of Fig. 1. The oxidation was produced by the addition of an amount of anaerobic ferricyanide slightly substoicheiometric with respect to the sum of the reduced metal centers. The H^+/COX ratio for H^+ release was calculated dividing the amount of H^+ release by the amount of COX oxidized. No pH changes were observed upon a second addition of the same amount of anaerobic ferricyanide. For other details, see Section 2.

the control, the H^+/COX ratio for proton release associated to anaerobic oxidation of the oxidase was depressed to 1.25. The mean values for these measurements are presented in panel A of Fig. 3. Oxidation of the unligated reduced oxidase by ferricyanide was associated with H^+ release in the external phase with an H^+/COX ratio which slightly decreased from around 1.7 to 1.6 as the pH was raised from 6.2 to 7.5 and then increased significantly upon further pH increase to around 2 at pH 8.4 (Fig. 3A, filled squares). This H^+ release results from deprotonation of COX protolytic groups whose pKs decrease upon oxidation of the COX redox centers. Zn^{2+} inhibited the H^+ release which now resulted in an H^+/COX ratio of 1.4–1.2 in the pH range 6.2–8.5 (Fig. 3A, empty squares).

Anaerobic oxidation by FIC of the CN^--ligated reduced oxidase, in which heme a_3 was clamped in the oxidized state, resulted in H^+ release from COV with an H^+/COX ratio which decreased from 1.3 at pH 6.2 to 0.8 at alkaline pHs (Fig. 3B, filled circles). At pH ≈ 8 the H^+/COX ratio for proton release was equal to that found in the CO-ligated oxidase in which only Cu_A and heme *a* undergo oxido-reduction (Fig. 3C, filled triangles). Zn^{2+} had no effect on ferricyanide induced H^+ release in the CN^--ligated oxidase (Fig. 3B, empty circles) and in the CO-ligated oxidase, in which heme a_3 and Cu_B are clamped in the reduced state (Fig. 3C) [21].

The effect of Zn^{2+} on the vectorial nature of the redox Bohr protons in COVs with unligated as well as CN^--ligated enzyme was then examined. The metal centers of the oxidase were fully pre-reduced by succinate using a trace of disrupted mitochondria and cytochrome *c*. In the unligated oxidase rapid oxidation of the metal centers by the addition of a stoichiometric amount of ferricyanide was accompanied by a synchronous release of protons (H_i^+) from COV which was practically the same as that measured in the experimental conditions of Fig. 2 (see $^*H^+$/COX in Table 2). Oxidation of the metal centers of the oxidase was followed by their slow rereduction by succinate, with chemical H^+ release deriving from succinate oxidation. Correction for this leaves a final amount of H^+ release in the external (P) space (H_f^+) (see Fig. 4). If H_f^+ is equal to H_i^+, the Bohr H^+ released in the external space, upon oxidation of the redox centers, are all taken up from the inner COV space, separated from the outer space by the relatively H^+ impermeable liposomal membrane. If, on the other hand, all the Bohr protons released outside upon oxidation of the metal centers are taken up from the same outer space, H_f^+ will be equal to zero. An eventual difference, H_i^+ minus H_f^+ (see Table 2) represents the fraction of scalar Bohr protons exchanged at the outer side of the oxidase and the residual H_f^+, the fraction of the vectorial Bohr protons.

In the unligated COV, internally bound Zn^{2+} depressed the initial H^+ release (H_i^+) associated with anaerobic oxidation of the oxidase but had no significant effect on the final amount of H^+ release in the outer space (H_f^+). Thus Zn^{2+} depressed the $H_i^+ - H_f^+$ difference, i.e., the scalar Bohr protons.

In the cyanide ligated oxidase (a_3 clamped in the oxidized state) the final H_f^+ release after the oxido-rereduction cycle was practically equal to the initial H_i^+ release. Thus, all the Bohr H^+ associated with the oxidation of heme *a*/Cu_A and Cu_B, amounting to ≈1.3 per oxidase molecule at pH 6.5 and suppressed by CCCP, are vectorial (Table 2), it is to say released in the external space upon oxidation of these metal centers and taken up from the inner space upon their rereduction (see also ref. [17,18]). The difference H_i^+/COX − H_f^+/COX observed only in the unligated oxidase, representing scalar Bohr protons exchanged at the outer surface, can thus be ascribed to oxidation/reduction of heme a_3. These scalar redox Bohr protons are depressed by Zn^{2+}.

4. Discussion

In liposome recostituted *P. denitrificans* cytochrome *c* oxidase, internally trapped Zn^{2+} was found to uncouple proton pumping associated with aerobic oxidation of ferrocytochrome *c*, with small effect on the rate of electron flow [28]. In the reconstituted *P. denitrificans* oxidase internally trapped Zn^{2+} also decelerated the rapid charge

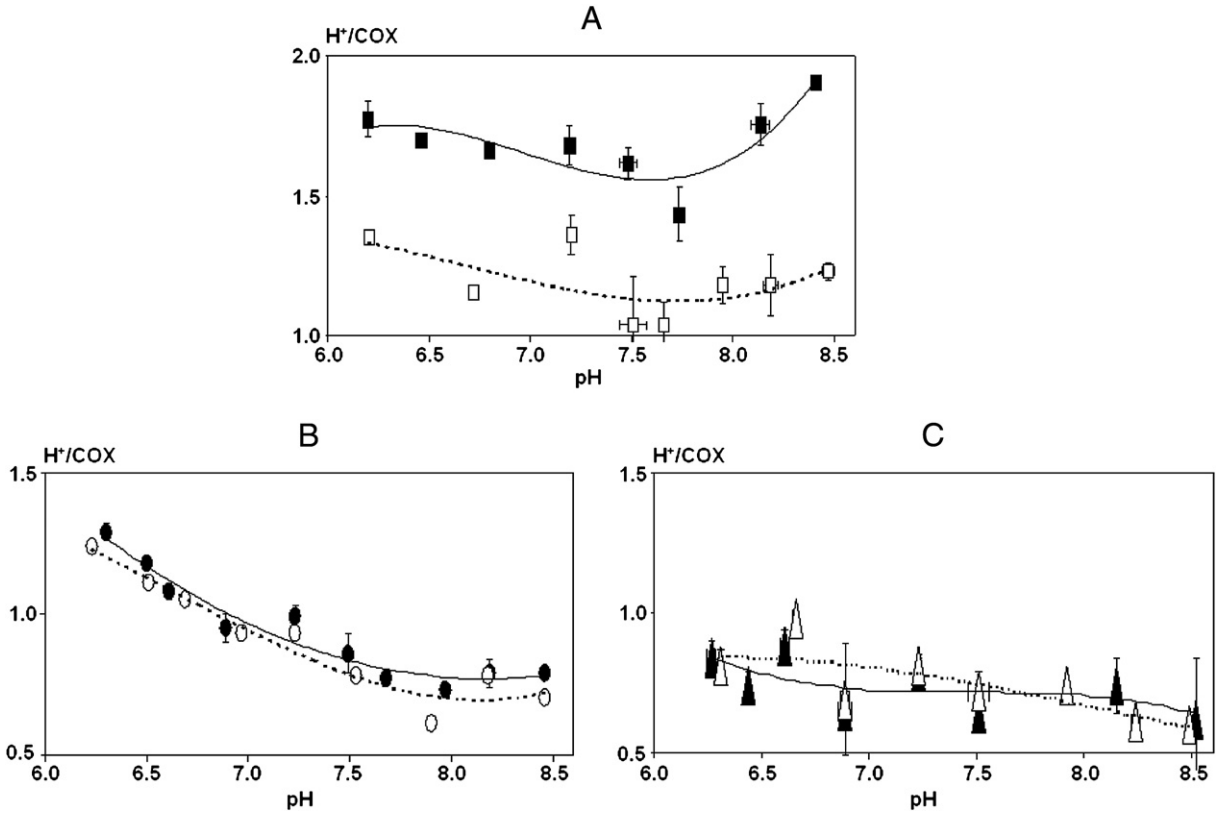

Fig. 3. pH dependence of proton release associated with ferricyanide anaerobic oxidation of unligated, CN-ligated and CO-ligated oxidase in COV. For anaerobic oxidation of unligated (A) and CO-ligated (C) COV (1–1.5 μM aa_3 plus 1.5 μM cytochrome *c*), the anaerobic reduction was produced by riboflavin/EDTA-mediated photoreduction (see legends to Figs. 1 and 2). In the case of CN-ligated enzyme (B) (2 μM aa_3, 2 μM cytochrome *c*), the anaerobic reduction was attained by 2 mM K–succinate in the presence of 0.05 mg/ml disrupted BHM and 0.5 μg rotenone/ml followed by the addition of 0.1 μM antimycin A and 0.3 μM myxothiazol. The oxidation was produced by the addition of an amount of anaerobic ferricyanide slightly substoicheiometric with respect to the sum of the reduced metal centers, these amounted in the unliganded COV, four times the amount of COX oxidized plus cytochrome *c*; in the CO-ligated COV, two times the measured COX oxidized plus added cytochrome *c*; in the CN-ligated COV, three times the amount of COX oxidized plus cytochrome *c*. The H^+/COX ratios reported were calculated dividing the amount of proton release by the amount of COX oxidized. Filled symbols refer to control COV, empty symbols to COV with 200 μM internally trapped Zn^{2+}. The values reported are the means ± S.E.M. from 1 to 5 different measurements under each condition. For other details, see Section 2.

displacement associated with proton uptake from the N space, in the electron transfer steps O → E and F → O of the oxidase catalytic cycle [28, cf. 29].

The present results show that in liposome reconstituted bovine heart cytochrome *c* oxidase internally trapped Zn^{2+} causes, under level flow conditions, 50% inhibition of proton pumping without effect

Table 2
Statistical analysis of the sidedness of H^+ transfer linked to redox transitions of the metal centers in reconstituted cytochrome *c* oxidase vesicles. Effect of internal Zn^{2+}.

Experimental conditions			pH	*H^+/COX	H_f^+/FIC	H_i^+/COX	H_f^+/COX	H_i^+/COX–H_f^+/COX
Unligated	Coupled	Control		1.68 ± 0.01 *(3)*	1.15 ± 0.01 *(9)*	1.60 ± 0.10 *(9)*	1.17 ± 0.08 *(9)*	0.43 ± 0.09
		+ Zn^{2+}		1.25 ± 0.10 *(2)*	1.17 ± 0.02 *(21)*	1.39 ± 0.04 *(21)*	1.24 ± 0.10 *(21)*	0.16 ± 0.06
			6.7					
	Uncoupled	Control			0.96 ± 0.03 *(9)*			
		+ Zn^{2+}			1.06 ± 0.03 *(7)*			
CN-ligated	Coupled	Control		1.29 ± 0.03 *(3)*	1.26 ± 0.01 *(9)*	1.37 ± 0.06 *(9)*	1.30 ± 0.04 *(9)*	
		+ Zn^{2+}		1.24 ± 0.19 *(2)*	1.24 ± 0.02 *(10)*	1.30 ± 0.02 *(10)*	1.23 ± 0.05 *(10)*	
			6.5					
	Uncoupled	Control			0.98 ± 0.05 *(4)*			
		+ Zn^{2+}			0.91 ± 0.03 *(4)*			

1.5 μM COV were suspended in 150 mM KCl and supplemented with 1.5 μM cytochrome *c*, 4 μM valinomycin, 0.05 mg/ml disrupted BHM, 1 μg/ml rotenone, 1 mM EDTA at the pH specified in the table. The pH changes associated with redox transitions of the metal centers in COX were measured potentiometrically and calibrated as in the legend to Table 1. Fully reduction of cytochrome *c* oxidase (and cytochrome *c*) was achieved in about 5 min by adding 2 mM succinate in the presence of the trace of BHM. *H/COX was from Fig. 2. H_f^+/FIC refers to the ratio between the total amount of H^+ released following the oxido-rereduction cycle elicited by the addition of ferricyanide and the amount of ferricyanide added. H_i^+/COX refers to the ratio between the initial proton release associated to the transient oxidation of metal centers and the amount of oxidized cytochrome *c* oxidase. H_f^+/COX refers to the ratio between the amount of protons, left in the external P space at the end of the oxidation–rereduction cycle, after correction for scalar protons derived from the oxidation of succinate by COX metal centers, and the amount of cytochrome *c* oxidase undergoing oxido-reduction (see Fig. 4 for experimental procedure). The values reported represent μM changes of measured COX oxidation and H^+ release and are means ± S.E.M. from *(n)* different experiments. The data of control COV in the unligated and CN^- inhibited COX, collected in set of experiments carried out by the authors are also reported in a recent review paper [18]. For other details, see Section 2.

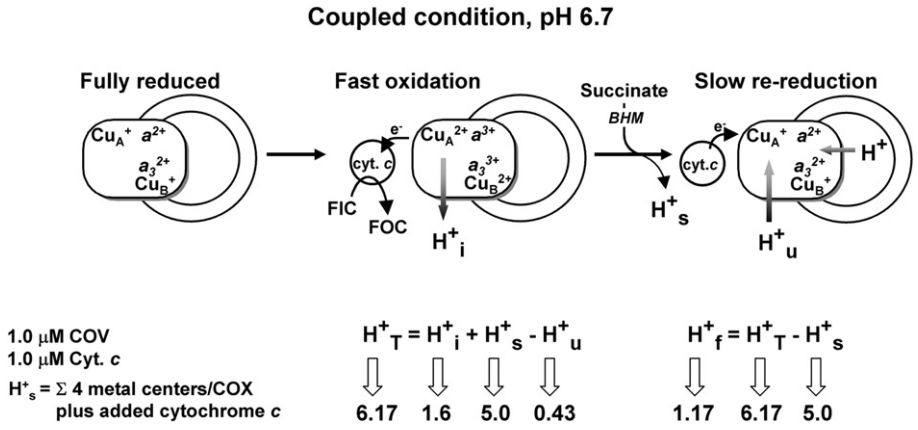

Fig. 4. Experimental scheme describing the membrane sidedness of H^+ transfer associated with redox transition of the metal centers in cytochrome *c* oxidase vesicles. The experimental conditions are described in the legend of Table 2. The values under each arrow refer to μM H^+ changes. Correction for the chemical H^+ release deriving from succinate oxidation amounts to the sum of the metal centers rereduced (four metal centers per COX plus added cytochrome *c*). For other details see legend of Table 2 and text.

on the steady-state rate of electron flow and the RCR. It has to be noted that in our experiments the overall rate of electron flow was determined by electron delivery to the oxidase, and amounted to ≈ 5 e^-/s/mol. This is around two orders lower than the maximal turnover of the enzyme. Under our experimental conditions partial inhibition of the rapid individual steps of the catalytic cycle does not result in inhibition of the overall rate of electron transfer as, instead, observed in the experiments by others [27,28], in which the rate of electron flow in the oxidase was set at values close to the maximal turnover of the oxidase.

The four proton pumping steps associated with the transfer of each of the four electrons in the protonmotive catalytic cycle of O_2 reduction to 2 H_2O have been found to be partitioned between the oxidative and the reductive phases of the catalytic cycle [35,48]. The relative contributions of the oxidative and reductive phases appear to be pH dependent: that of the oxidative phase decreases and that of the reductive phase increases with pH (Fig. 1, see also refs. [24,44]. At alkaline pHs, the two halves of the catalytic cycle contribute equally to proton pumping [35,44]. The opposite pH dependence of proton release in the oxidative and reductive phases of the proton pump cycle reflects that found for the pH dependence of scalar H^+ consumption for water formation in the oxidative and reductive phases of the oxygen reduction cycle in the soluble oxidase [49].

The steps of catalytic cycle of oxidase and of the associated proton translocations are schematically presented in Fig. 5. At the respiring steady state the catalytic cycle starts with the fully oxidized oxidase [24]. It is assumed that at physiological N-side alkaline pH, two OH^- are bound at the binuclear site [24,49]. It has been shown that it is the inner space pH, higher than 7.4 under steady-state conditions in mitochondria to determine the rates of electron and proton transfer in the oxidase [50]. Upon transfer of two electrons from ferrocytochrome *c* to heme a_3/Cu_B, one at a time via Cu_A/heme *a*, with generation of the mixed valence (MV) intermediate, the two OH^- are protonated to 2 H_2O by 2 H^+, normally taken up from the N space by the K proton conducting pathway [9–11,51]. At the same time of H_2O formation 2 H^+ are pumped from the N to the P space. O_2 upon binding at the reduced binuclear center, undergoes reductive cleavage [9,11,52,53]. Two electrons come from the oxidation of Fe^{2+}_{a3} to Fe^{4+}_{a3}, one from Cu^{1+}_B and the fourth, together with a chemical proton, from a tyrosine residue, with generation of the PM intermediate. The transfer of the third electron via Cu_A/heme *a* to the binuclear site, conversion of the PM to the F intermediate, results in the uptake of two H^+ from the N space. One H^+, together with the electron converts the tyrosine radical to protonated tyrosine, the other H^+ is pumped into the P space [53]. The transfer of the fourth electron via Cu_A/heme *a* to the binuclear center, which converts the F to the O intermediate is associated with the uptake of 2 H^+ from the N space. One is the fourth chemical proton utilized in the conversion of $Fe^{4+}_{a3}=O$ to Fe^{3+}_{a3}-OH^-, which, like the third, is conducted by the D pathway [9–11], the other is the fourth pumped H^+[10,53].

The present results indicate that the partial decoupling of proton pumping caused by internally bound Zn^{2+} is due to suppression of the release in the P space of the two pumped protons taking place when OH^- at the binuclear center site is protonated to H_2O. At acidic pH, where one of the two H_2O molecules is already formed in the oxidative phase of the cycle [49], Zn^{2+} did lower, from around 3.0 to 2.0, the H^+/COX ratio for proton release in the aerobic oxidation of the fully reduced COV. The proton release detected in the anaerobic reduction of the fully oxidized COV, which increased progressively with pH, was suppressed by Zn^{2+}.

Each of the four protons pumped in the electron transfer from ferrocytochrome *c* to the oxygen reduction center, is proposed to be mediated by redox Bohr coupling at heme *a* (Cu_A) [17,18,24, see also 25]. Redox cycling of heme *a* will be responsible for the transfer of pumped protons from the N-side to the pump site (C_1 cluster), from which they are then released in the P space [18]. The acid–base groups contributing to the C_1 cluster remain to be defined. The C_1 cluster, likely contributed by Arg38 of subunit I (bovine numbering), hydrogen bonded to the formyl substituent of heme *a*[14,16,22], can be extended by a hydrogen bond network, involving a conserved arginine (Arg-I438 bovine numbering) and the Δ-propionates of heme *a* and heme a_3[54]. The structure of this network may be critical in preventing annihilation of pumped protons in the formation of H_2O at the binuclear site.

The redox Bohr effect coupled to heme *a* is the net result of proton transfer in a cluster of protolytic groups in the oxidase [18,23,55,56]. The expected net charge displacement along the axis perpendicular to the membrane plane can be minimized by H^+ transfer along multiple protolytic groups located at small distances perpendicular to the plane of the membrane, without significant generation of a transmembrane voltage, in addition to that generated by fast electron flow from Cu_A to heme *a*[23]. This step is then followed by slower electrogenic proton transfer from the N space to the C_1 cluster, at the same time of electron transfer from heme *a* to the binuclear site and final release of H^+ from the C_1 cluster in the P space [23]. Direct analysis of the mixed valence carbon-monoxide ligated oxidase, in which heme a_3 and Cu_B are clamped in the reduced state, shows that Zn^{2+} has no effect on redox Bohr protons associated with anaerobic oxido-reduction of heme *a* (and Cu_A) (Fig. 3). Neither Zn^{2+} had any effect on vectorial Bohr

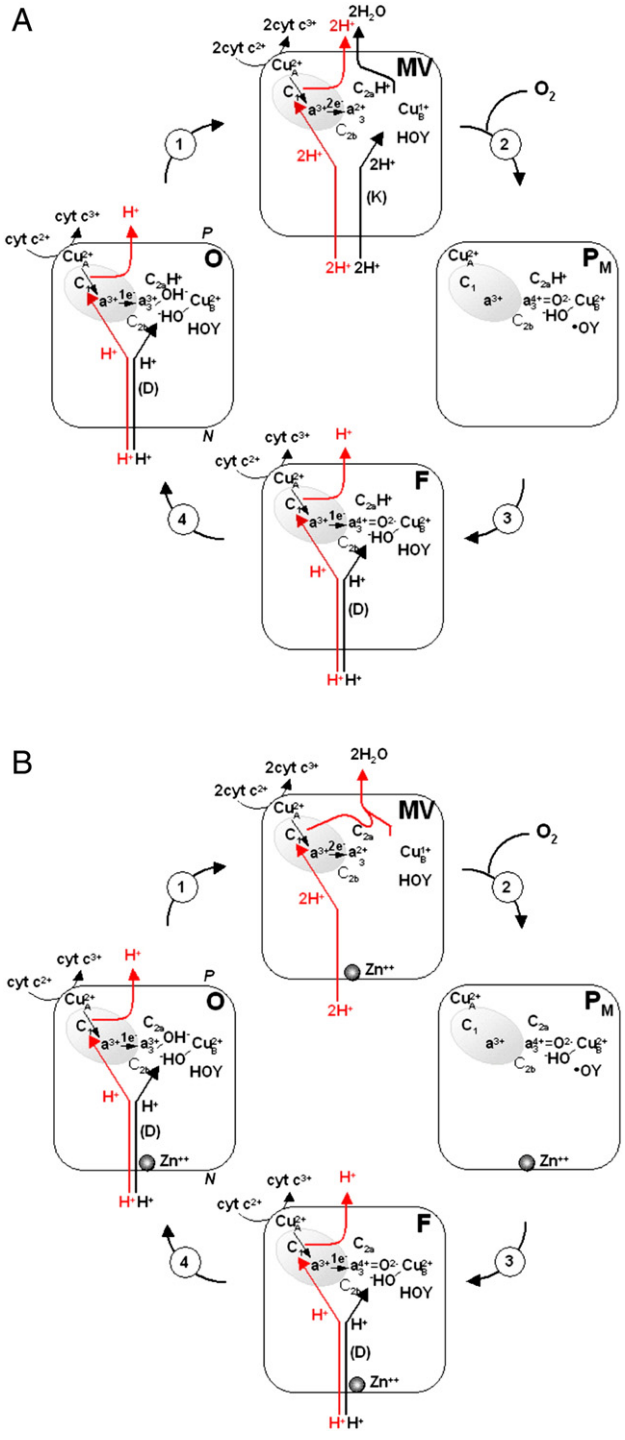

Fig. 5. Scheme of the proton pumping steps in the oxygen reduction catalytic cycle of cytochrome *c* oxidase in the steady-state physiological respiring condition (A) and in the presence of internally bound Zn^{2+} (B). O, MV, P_M and F represent the main catalytic intermediates of the oxygen reduction cycle at the heme a_3–Cu_B and the nearby Y244 reaction site [11]. Red and black arrows indicate vectorial and scalar proton transfer respectively through proton channels in the transitions from O to MV, P_M to F and F to O respectively. C_1 indicates a cluster of acid–base groups whose pKs are linked to redox transitions of Cu_A/heme *a*. C_{2a} and C_{2b} indicate clusters of acid–base groups whose pKs are linked to redox transitions of heme a_3 and Cu_B, respectively. The cycle refers to a condition of alkaline pH. See Section 4 for further details.

protons associated with oxido-reduction of the CN-inhibited oxidase in which heme a_3 is clamped in the oxidized state (Table 2, Fig. 3). The inhibitory effect of Zn^{2+} on Bohr protons observed in the unligated oxidase can, therefore, be ascribed to inhibition of Bohr protons exchanged at the external P-side upon oxido-reduction of heme a_3. The numbers of these scalar protons (H_i^+-H_f^+ in Table 2) can also be calculated from the difference of the H^+ release from COV, measured upon anaerobic oxidation of the unligated oxidase and the H^+ release measured in the CN-ligated oxidase (panels A and B in Fig. 3). This calculation shows that the number of Bohr protons associated to heme a_3 increases with pH from ≈0.6 at pH 6.2 to ≈1.2 at pH 8.4 (H^+/COX ratios in panel A minus H^+/COX ratios in panel B of Fig. 3, see also [18]). These scalar Bohr protons, detected only in the anaerobic ferricyanide oxidation of the fully reduced COV are a sign of redox-linked stereochemical change of a residue cluster linked to heme a_3.

In the turning over oxidase, upon reduction of the oxidized enzyme two OH^- are protonated to two H_2O at the same time that two electrons are transferred to the site, and kept in the oxygen reduction intermediates, together with two other electrons subsequently delivered from cytochrome *c*, till 2 H_2O leave the site. Under these conditions the residue cluster coupled to heme a_3 can be kept protonated throughout the cycle, in a protein conformation that prevents annihilation of the pumped protons in the formation of H_2O. Extended X-ray absorption spectroscopy (EXAFS) has revealed tetra-coordination site(s) for Zn^{2+} in the isolated bovine heart cytochrome *c* oxidase with two nitrogens of histidine imidazoles, one nitrogen of histidine imidazol or lysine and one oxygen of glutamate or aspartate carboxylic group, likely located at the entry site of the proton conducting D pathway in the oxidase [33]. Zn^{2+} binding residues exposed at the entrance site of the D pathway have been, directly, identified by the X-ray crystallographic structure of the bovine oxidase [34]. These are His 503 and Glu 506 of subunit I, His 2, Glu 5 and Lys 9 of subunit VIIc and His 3 of subunit III, which contribute, in various combinations, to tetra-coordination of Zn^{2+}.

It is proposed that internal (N-side) binding of Zn^{2+}, likely at the entry mouth of the D channel, in addition to deceleration of the rapid H^+ uptake from the N space, associated to the electron transfer steps O → E, P → F and F → O [28,29], also results in a conformational change in the protein environment of heme a_3, which normally prevents annihilation of pumped protons in the formation of H_2O. Upon alteration of this barrier by Zn^{2+} binding, the two protons which, in the reduction of the O to the MV intermediate, are taken from the N space by the pump input channel (D [9–11] or H [2,14] channel in the bovine oxidase), instead of being finally released in the P space are consumed in the protonation of 2 OH^- to 2 H_2O, thus replacing utilization of protons conducted by the K pathway (see Fig. 5). For the relationship of the model in Fig. 5 to the model of Yoshikawa's group [14,34] and to different models of Wikstrom/Verkhovsky [12,25] and Brzezinski et al. [11,13] see our recent review paper [18].

Acknowledgements

This work was supported by the National Project, "Progetto FIRB Rete Nazionale per lo studio della Proteomica Umana (Italian Human ProteomeNet)", 2009, Ministero dell'Istruzione, dell'Università e della Ricerca (MIUR) and University of Bari Research grant, 2009.

We gratefully acknowledge contribution of Dr. F. Francia for determination of internal Zn^{2+} concentration in COV.

References

[1] S. Iwata, C. Ostermeier, B. Ludwig, H. Michel, Structure at 2.8 Å resolution of cytochrome *c* oxidase from *Paracoccus denitrificans*, Nature 376 (1995) 660–669.
[2] T. Tsukihara, H. Aoyama, E. Yamashita, T. Tomizaki, H. Yamaguchi, K. Shinzawa-Itoh, R. Nakashima, R. Yaono, S. Yoshikawa, The whole structure of the 13-subunit oxidized cytochrome *c* oxidase at 2.8 Å, Science 272 (1996) 1136–1144.
[3] P. Mitchell, Chemiosmotic coupling and energy transduction, Glynn Research, Bodmin (1968).

[4] S. Papa, Proton translocation reactions in the respiratory chain, Biochim. Biophys. Acta 456 (1976) 39–84.
[5] M. Wikstrom, K. Krab, M. Saraste, Proton-translocating cytochrome complexes, Ann. Rev. Biochem. 50 (1981) 623–655.
[6] N. Capitanio, G. Capitanio, D.A. Demarinis, E. De Nitto, S. Massari, S. Papa, Factors affecting the H^+/e^- stoichiometry in mitochondrial cytochrome *c* oxidase: influence of the rate of electron flow and transmembrane delta pH, Biochemistry 35 (1996) 10800–10806.
[7] S. Papa, F. Guerrieri, M. Lorusso, S. Simone, Proton translocation and energy transduction in mitochondria, Biochimie 55 (1973) 703–716.
[8] M.M. Pereira, C.M. Gomes, M. Teixeira, Plasticity of proton pathways in haem-copper oxygen reductases, FEBS Lett. 522 (2002) 14–18.
[9] S. Ferguson-Miller, G.T. Babcock, Heme/copper terminal oxidases, Chem. Rev. 96 (1996) 2889–2908.
[10] A.A. Konstantinov, S. Siletsky, D. Mitchell, A. Kaulen, R.B. Gennis, The roles of the two proton input channels in cytochrome *c* oxidase from *Rhodobacter sphaeroides* probed by the effects of site-directed mutations on time-resolved electrogenic intraprotein proton transfer, Proc. Natl. Acad. Sci. U.S.A. 94 (1997) 9085–9090.
[11] G. Branden, R.B. Gennis, P. Brzezinski, Transmembrane proton translocation by cytochrome *c* oxidase, Biochim. Biophys. Acta 1757 (2006) 1052–1063.
[12] M. Wikstrom, Cytochrome *c* oxidase: 25 years of the elusive proton pump, Biochim. Biophys. Acta 1655 (2003) 241–247.
[13] K. Faxèn, G. Gilderson, P. Ädelroth, P. Brzezinski, A mechanistic principle for proton pumping by cytochrome c oxidase, Nature 437 (2005) 286–289.
[14] S. Yoshikawa, K. Shinzawa-Itoh, R. Nakashima, R. Yaono, E. Yamashita, N. Inoue, M. Yao, M.J. Fei, C.P. Libeu, T. Mizushima, H. Yamaguchi, T. Tomizaki, T. Tsukihara, Redox-coupled crystal structural changes in bovine heart cytochrome *c* oxidase, Science 280 (1998) 1723–1729.
[15] V.Y. Artzatbanov, A.A. Konstantinov, V.P. Skulachev, Involvement of intramitochondrial protons in redox reactions of cytochrome alpha, FEBS Lett. 87 (1978) 180–185.
[16] G.T. Babcock, P.M. Callahan, Redox-linked hydrogen bond strength changes in cytochrome a: implications for a cytochrome oxidase proton pump, Biochemistry 22 (1983) 2314–2319.
[17] N. Capitanio, G. Capitanio, E. De Nitto, S. Papa, Vectorial nature of redox Bohr effects in bovine heart cytochrome *c* oxidase, FEBS Lett. 414 (1997) 414–418.
[18] G. Capitanio, P.L. Martino, N. Capitanio, S. Papa, Redox Bohr effects and the role of heme *a* in the proton pump of bovine heart cytochrome *c* oxidase, Biochim. Biophys. Acta (2011) Epub ahead of print.
[19] S. Papa, N. Capitanio, G. Villani, A cooperative model for protonmotive heme-copper oxidases. The role of heme a in the proton pump of cytochrome c oxidase, FEBS Lett. 439 (1998) 1–8.
[20] H. Michel, Cytochrome *c* oxidase: catalytic cycle and mechanisms of proton pump – a discussion, Biochemistry 38 (1999) 15129–15140.
[21] N. Capitanio, G. Capitanio, M. Minuto, E. De Nitto, L.L. Palese, P. Nicholls, S. Papa, Coupling of electron transfer with proton transfer at heme *a* and Cu_A (redox Bohr effects) in cytochrome *c* oxidase. Studies with the carbon monoxide inhibited enzyme, Biochemistry 39 (2000) 6373–6379.
[22] T. Tsukihara, K. Shimokata, Y. Katayama, H. Shimada, K. Muramoto, H. Aoyama, M. Mochizuki, K. Shinzawa-Itoh, E. Yamashita, M. Yao, Y. Ishimura, S. Yoshikawa, The low-spin heme of cytochrome *c* oxidase as the driving element of the proton-pumping process, Proc. Natl. Acad. Sci. U.S.A. 100 (2003) 15304–15309.
[23] S. Papa, N. Capitanio, G. Capitanio, A cooperative model for proton pumping in cytochrome *c* oxidase, Biochim. Biophys. Acta 1655 (2004) 353–364.
[24] S. Papa, G. Capitanio, P.L. Martino, Concerted involvement of cooperative proton-electron linkage and water production in the proton pump of cytochrome *c* oxidase, Biochim. Biophys. Acta 1757 (2006) 1133–1143.
[25] I. Belevich, D.A. Bloch, N. Belevich, M. Wikstrom, M.I. Verkhovsky, Exploring the proton pump mechanism of cytochrome c oxidase in real time, Proc. Natl. Acad. Sci. U.S.A. 104 (2007) 2685–2690.
[26] P. Nicholls, A.P. Singh, Effect of zinc on proteoliposomal cytochrome oxidase, Life Sci. Adv. (Biochemistry, Delhi) 7 (1988) 321–326.
[27] S.S. Kuznetsova, N.V. Azarkina, T.V. Vygodina, S.A. Siletsky, A.A. Konstantinov, Zinc ions as cytochrome *c* oxidase inhibitors: two sites of action, Biochemistry (Moscow) 70 (2005) 128–136.
[28] A. Kannt, T. Ostermann, H. Müller, M. Ruitenberg, Zn^{2+} binding to the cytoplasmic side of Paracoccus *denitrificans* cytochrome *c* oxidase selectively uncouples electron transfer and proton translocation, FEBS Lett. 503 (2001) 142–146.
[29] A. Aagaard, P. Brzezinski, Zinc ions inhibit oxidation of cytochrome *c* oxidase by oxygen, FEBS Lett. 494 (2001) 157–160.
[30] K. Faxen, L. Salomonsson, P. Adelröth, P. Brzezinski, Inhibition of proton pumping by zinc ions during specific reaction steps in cytochrome *c* oxidase, Biochim. Biophys. Acta 1757 (2006) 388–394.
[31] D.A. Mills, B. Schmidt, C. Hiser, E. Westley, S. Ferguson-Miller, Membrane potential-controlled inhibition of cytochrome *c* oxidase by zinc, J. Biol. Chem. 277 (2002) 14894–14901.
[32] T.V. Vygodina, W. Zakirzianova, A.A. Konstantinov, Inhibition of membrane-bound cytochrome *c* oxidase by zinc ions: high-affinity Zn^{2+}-binding site at the P-side of the membrane, FEBS Lett. 582 (2008) 4158–4162.
[33] F. Francia, L. Giachini, F. Boscherini, G. Venturoli, G. Capitanio, P.L. Martino, S. Papa, The inhibitory binding site(s) of Zn^{2+} in cytochrome *c* oxidase, FEBS Lett. 581 (2007) 611–616.
[34] K. Muramoto, K. Hirata, K. Shinzawa-Itoh, S. Yoko-o, E. Yamashita, H. Aoyama, T. Tsukihara, S. Yoshikawa, A histidine residue acting as a controlling site for dioxygen reduction and proton pumping by cytochrome *c* oxidase, Proc. Natl. Acad. Sci. U.S.A. 104 (2007) 7881–7886.
[35] D. Bloch, I. Belevich, A. Jasaitis, C. Ribacka, A. Puustinen, M.I. Verkhovsky, M. Wikstrom, The catalytic cycle of cytochrome *c* oxidase is not the sum of its two halves, Proc. Natl. Acad. Sci. U.S.A. 101 (2004) 529–533.
[36] B. Errede, M.O. Kamen, Y. Hatefi, Preparation and properties of complex IV (ferrocytochrome *c*: oxygen oxidoreductase EC 1.9.3.1), Methods Enzymol. 53 (1978) 40–47.
[37] B. Kadenbach, M. Ungibauer, J. Jarausch, U. Buge, L. Kuhn-Nentwig, The complexity of respiratory complexes, Trends Biochem. Sci. 8 (1983) 398–400.
[38] P. Nicholls, Effects of inhibitory ligands on the aerobic carbon monoxide complex of cytochrome c oxidase, Biochem. J. 183 (1979) 519–529.
[39] T. Soulimane, G. Buse, Integral cytochrome *c* oxidase: preparation and progress towards a three-dimensional crystallization, Eur. J. Biochem. 227 (1995) 588–595.
[40] S. Yoshikawa, M. Mochizuki, X.J. Zhao, W.S. Caughey, Effect of overall oxidation state on infrared spectra of heme a_3 cyanide in bovine heart cytochrome *c* oxidase, J. Biol. Chem. 270 (1995) 4270–4279.
[41] S. Papa, F. Capuano, M. Markert, N. Altamura, The H^+/O stoicheiometry of mitochondrial respiration, FEBS Lett. 111 (1980) 243–248.
[42] N. Capitanio, G. Capitanio, E. De Nitto, G. Villani, S. Papa, H^+/e^-stoichiometry of mitochondrial cytochrome complexes reconstituted in liposomes, FEBS Lett. 288 (1991) 179–182.
[43] S. Papa, F. Guerrieri, G. Izzo, Cooperative proton-transfer reactions in the respiratory chain: redox Bohr effects, Methods Enzymol. 126 (1986) 331–343.
[44] G. Capitanio, P.L. Martino, N. Capitanio, E. De Nitto, S. Papa, pH dependance of proton translocation in the oxidative and reductive phases of the catalytic cycle of cytochrome c oxidase. The role of H_2O produced at the oxygen-reduction site, Biochemistry 45 (2006) 1930–1937.
[45] M.I. Verkhosvky, J.E. Morgan, M. Wikstrom, Control of electron delivery to the oxygen reduction site of cytochrome *c* oxidase: a role for protons, Biochemistry 34 (1995) 7483–7491.
[46] W.H. Vanneste, The stoichiometry and absorption spectra of components *a* and a_3 in cytochrome *c* oxidase, Biochemistry 5 (1966) 838–848.
[47] R. Traber, H.E.A. Kramer, P. Hemmerich, Mechanism of light-induced reduction of biological redox centers by aminoacids. A flash photolysis study of flavin photoreduction by ethylendiaminetetraacetate and nitriloacetate, Biochemistry 21 (1982) 1687–1693.
[48] M.I. Verkhovsky, A. Jasaitis, M.L. Verkhovskaya, J.E. Morgan, M. Wikstrom, Proton translocation by cytochrome *c* oxidase, Nature 400 (1999) 480–483.
[49] N. Capitanio, G. Capitanio, E. De Nitto, D. Boffoli, S. Papa, Proton transfer reactions associated with the reaction of the fully reduced, purified cytochrome *c* oxidase with molecular oxygen and ferricyanide, Biochemistry 42 (2003) 4607–4612.
[50] K. Faxen, P. Brzezinski, The inside pH determines rates of electron and proton transfer in vesicle-reconstituted cytochrome c oxidase, Biochim. Biophys. Acta 1767 (2007) 381–386.
[51] M. Ruitenberg, A. Kannt, E. Bamberg, B. Ludwig, H. Michel, K. Fendler, Single-electron reduction of the oxidized state is coupled to proton uptake via the K pathway in Paracoccus denitrificans cytochrome *c* oxidase, Proc. Natl. Acad. Sci. U.S.A. 97 (2000) 4632–4636.
[52] T. Kitagawa, T. Ogura, Oxygen activation mechanism at the binuclear site of heme-copper oxidase superfamily as revealed by time-resolved Raman spectroscopy, Prog. Inorg. Chem. 45 (1997) 431–479.
[53] P. Brzezinski, G. Larsson, Redox-driven proton pumping by heme-copper oxidases, Biochim. Biophys. Acta 1605 (2003) 1–13.
[54] T. Egawa, H.J. Lee, R.B. Gennis, S.R. Yeh, D.L. Rousseau, Critical structural role of R481 in cytochrome *c* oxidase from *Rhodobacter sphaeroides*, Biochim. Biophys. Acta 1787 (2009) 1272–1275.
[55] A.V. Xavier, Thermodynamic and choreographic constraints for energy transduction by cytochrome *c* oxidase, Biochim. Biophys. Acta 1658 (2004) 23–30.
[56] A. Kannt, L.R.D. Lancaster, H. Michel, The coupling of electron transfer and proton translocation: electrostatic calculations on *Paracoccus denitrificans* cytochrome *c* oxidase, Biophys. J. 74 (1998) 708–721.